

# Calcium Signaling in Dendrites and Spines: Practical and Functional Considerations

Michael J. Higley<sup>1</sup> and Bernardo L. Sabatini<sup>1,\*</sup>

<sup>1</sup>Howard Hughes Medical Institute, Department of Neurobiology, Harvard Medical School, 220 Longwood Avenue, Boston, MA 02115, USA

\*Correspondence: [bernardo\\_sabatini@hms.harvard.edu](mailto:bernardo_sabatini@hms.harvard.edu)

DOI 10.1016/j.neuron.2008.08.020

Changes in intracellular calcium (Ca) concentration following synaptic and suprathreshold activity are mediated by a wide range of sources and contribute to the regulation of myriad neuronal functions. The development of Ca imaging techniques has dramatically increased our understanding of the complex interactions between different Ca sources and their ability to produce spatial and temporal specificity of signaling, even within small cellular compartments such as dendrites and dendritic spines. However, as the use of Ca imaging has become more prevalent, the need to exercise care in the experimental methodology and interpretation of data has also grown. In this review, we discuss the recent progress made using imaging methods in understanding dendritic Ca signaling and also describe a quantitative framework for using fluorescent indicators to experimentally measure and interpret changes in intracellular Ca.

Calcium (Ca) influx into the cytoplasm of dendrites and dendritic spines regulates a variety of neuronal functions, including synaptic signaling, induction of short- and long-term plasticity, and regulation of gene transcription (reviewed in Sabatini et al., 2001; Soderling, 2000; Zucker, 1999). Ca accumulation within these structures is evoked by action potentials and synaptic stimuli, which generate Ca influx through multiple classes of ion channels as well as release from internal stores. The dynamics of evoked Ca signals depend on the properties of the stimulus, the local membrane potential, and recent patterns of activity. Furthermore, nonlinear interactions between Ca sources produce a complexity of signaling that allows this ubiquitous second messenger to act with surprising spatial and temporal specificity. The development of optical methods for measuring changes in intracellular Ca concentration has allowed unprecedented access to the biochemical signaling events that occur inside small cellular compartments such as dendrites and spines. Here, we first review recent progress in understanding the factors influencing Ca signaling within dendritic compartments. We then discuss a quantitative framework for experimentally measuring and interpreting changes in intracellular Ca through the use of fluorescent indicators.

## Section I. Ca Signaling in Neuronal Dendrites and Spines

In this section, we will review recent work illustrating how optical methods of measuring Ca influx have provided insight into Ca signaling in dendrites and spines of central neurons. We will limit our discussion to postsynaptic Ca handling in principal cells and focus primarily on those papers that have used imaging methods to directly measure Ca dynamics in specific subcellular compartments.

### Postsynaptic Calcium Sources

Synaptically evoked increases in cytoplasmic Ca arise from three general sources: glutamate receptors, voltage-sensitive Ca channels (VSCCs), and release from internal stores (see Fig-

ure 1). The specific contributions made by each of these depend considerably on the brain structure, cell class, and even subcellular compartment. Glutamate receptors, consisting broadly of NMDA-type (NMDARs) and non-NMDA-type receptors, are found throughout the central nervous system on dendritic shafts and spines of multiple cell classes (Cowan et al., 2001). NMDARs contribute a significant fraction of synaptic Ca influx in a variety of cells, including pyramidal neurons in both the CA1 (Bloodgood and Sabatini, 2007; Kovalchuk et al., 2000; Mainen et al., 1999; Müller and Connor, 1991; Regehr and Tank, 1992; Sobczyk et al., 2005; Yuste et al., 1999) and CA3 (Reid et al., 2001) regions of the hippocampus, cortical spiny stellate (Nevian and Sakmann, 2004) and pyramidal neurons (Koester and Sakmann, 1998; Schiller et al., 1998), striatal medium spiny neurons (Carter and Sabatini, 2004; Carter et al., 2007), and olfactory granule cells (Egger et al., 2005). The conductance of cations, including Ca, through NMDARs is strongly regulated by membrane potential due to pore blockade by extracellular magnesium (Mg) ions (Nowak et al., 1984). However, even at the resting potentials of most cells, Mg block is incomplete, and glutamate binding to NMDARs can evoke Ca influx in the absence of additional depolarization (Jahr and Stevens, 1990; Sabatini et al., 2002).

Although most non-NMDA-type glutamate receptors exhibit minimal Ca permeability, AMPA-type glutamate receptors (AMPA) lacking a GluR2 subunit are Ca permeable and have been primarily described in GABAergic interneurons (Burnashev et al., 1992; Cull-Candy et al., 2006). However, Ca influx via AMPARs has also been directly demonstrated in striatal medium spiny projection neurons (Carter and Sabatini, 2004) and has been inferred through pharmacological and physiological studies in hippocampal pyramidal neurons (Plant et al., 2006; Thiagarajan et al., 2005) and cerebellar Purkinje cells (Denk et al., 1995). Additionally, AMPARs contribute to Ca signaling by providing membrane depolarization, activating VSCCs (see below), and relieving Mg block from NMDARs (Bloodgood and

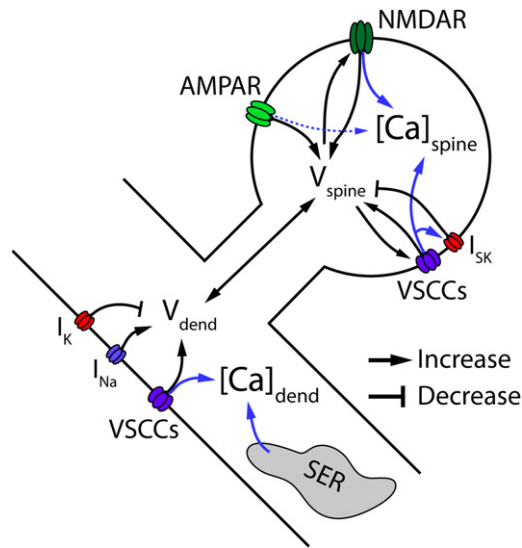


**Figure 1. Schematic Illustrating the Interplay of Ca Sources in Dendritic Shafts and Spines**

Synaptic activation produces local depolarization (black arrows) and Ca influx (blue arrows) via AMPARs and NMDARs. Depolarization enhances the conductance of NMDARs and activates VSCCs, contributing additional depolarization and augmenting Ca entry. In some cell classes, synaptic activation can also produce Ca release from internal stores such as the smooth endoplasmic reticulum (SER). Release from internal stores is depicted in the dendritic shaft but may also contribute to spine Ca signals. Dendritic depolarization produced by distal synaptic input or back-propagating action potentials can lead to local Ca influx via VSCCs and also boost depolarization in spines. Local membrane conductances, including sodium and potassium channels, can modulate Ca influx by regulating the local membrane potential. Finally, VSCCs (specifically, R-type channels) and SK-type Ca-activated potassium channels participate in a local feedback loop, illustrating the existence of nanodomain signaling within single dendritic compartments.

Sabatini, 2007; Denk et al., 1995; Nevian and Sakmann, 2004; Reid et al., 2001).

Another significant contributor to dendritic Ca signaling are VSCCs, which comprise a broad class of membrane channels with a wide variety of voltage dependence, activation, and inactivation properties (Hille, 2001). Within dendrites and spines, VSCCs open following strong synaptically evoked depolarization arising from the coactivation of many synapses (Christie et al., 1995; Denk et al., 1995; Eilers et al., 1995; Finch and Augustine, 1998; Magee et al., 1995; Markram and Sakmann, 1994; Miyakawa et al., 1992; Regehr and Tank, 1992; Reid et al., 2001; Schiller et al., 1998; Yuste and Denk, 1995). Sufficient depolarization for VSCC activation can also be provided by the back-propagation of somatically generated action potentials (bAPs) that spread antidromically through at least the proximal portions of the dendritic arbor (Bloodgood and Sabatini, 2007; Callaway and Ross, 1995; Carter and Sabatini, 2004; Helmchen et al., 1999; Koester and Sakmann, 2000; Nevian and Sakmann, 2004; Schiller et al., 1995; Svoboda et al., 1997; Waters et al., 2003; Yuste and Denk, 1995).

Fluorescent Ca imaging has been used in combination with pharmacological assays to reveal the extensive variation in VSCC subtypes active across different cell classes and within different subcellular compartments. In CA1 pyramidal neurons, Ca influx to dendritic shafts occurs via L-type, R-type, and low-

threshold T-type VSCCs (Christie et al., 1995; Magee et al., 1995; Sabatini and Svoboda, 2000), whereas influx into individual spine heads appears to be primarily limited to R-type channels with a small contribution from L-type channels (Bloodgood and Sabatini, 2007; Hoogland and Saggau, 2004; Sabatini and Svoboda, 2000; Yasuda et al., 2003). In cortical pyramidal neurons, dendritic VSCCs include L-type, N-type, P/Q-type, and R-type channels (Markram et al., 1995), while L-type, P/Q-type, and low-threshold T-type channels are found in spines (Koester and Sakmann, 2000). T-type VSCCs also contribute to dendritic Ca signals in both olfactory granule cells (Egger et al., 2005) and cerebellar Purkinje cells (Isope and Murphy, 2005). Within striatal medium spiny neurons, Ca influx occurs through L-type, R-type, and T-type channels in both dendritic shafts and spines (Carter and Sabatini, 2004). Interestingly, electron microscopy has demonstrated that L-type channels in MSN spines consist of the  $\alpha 1D$  subunit-containing  $CaV_{1.3}$  subtype (Day et al., 2006). These channels are activated at lower thresholds and are more resistant to block by dihydropyridines compared with  $CaV_{1.2}$  L-type channels (Lipscombe et al., 2004), making them difficult to distinguish pharmacologically from R-type channels and suggesting that earlier reports of R-type channel exclusivity may need to be revisited. The potentially imprecise mapping between pharmacological sensitivity and VSCC  $\alpha$  subunit expression makes the molecular composition of the channels mediating dendritic and spine Ca influx difficult to establish (Doering and Zamponi, 2003; Lipscombe et al., 2004).

The contributions of Ca release from internal stores to dendritic and spine Ca transients following synaptic activation are controversial. Using organotypic hippocampal slice cultures, Emptage et al. (1999) found that Ca-induced Ca release significantly contributed to synaptically evoked Ca transients in dendritic spines. Furthermore, in acute hippocampal CA1 slices, strong afferent stimulation can lead to activation of metabotropic glutamate receptors (mGluRs), triggering a phospholipase C (PLC)- and inositol triphosphate (IP<sub>3</sub>)-dependent Ca release from internal stores and contributing to long-term heterosynaptic plasticity (Dudman et al., 2007; Hong and Ross, 2007; Watanabe et al., 2006). However, other studies have failed to find evidence for Ca release from internal stores following more limited synaptic stimulation of hippocampal afferents (Kovalchuk et al., 2000; Mainen et al., 1999; Yuste et al., 1999). More evidence for synaptically evoked Ca release from internal stores exists for cerebellar Purkinje cells, where several groups have shown that activation of parallel fiber inputs can lead to Ca release via an mGluR-PLC-IP<sub>3</sub>-coupled pathway (Finch and Augustine, 1998; Miyata et al., 2000; Takechi et al., 1998; Wang et al., 2000).

### Mechanisms of Specificity in Ca Signaling

In light of the considerable diversity of spatially overlapping Ca sources, a key question has emerged: how is specificity of signaling achieved and maintained? Recent studies have suggested two potentially complementary solutions. First, considerable work has shown that Ca signaling can be spatially restricted, both at the nanoscale (~10–100 nm) and microscale (~1–100  $\mu$ m), providing biochemical signals that are limited to specific subcellular compartments. Second, due to the biophysical properties of many Ca sources (e.g., the voltage

dependence of NMDARs and VSCCs), Ca influx may herald various forms of coincidence detection, providing a signal that is generated only by specific patterns of neuronal activity.

### Signaling Specificity via Calcium Nanodomains

The compartmentalization of Ca signaling within nanodomains was initially suggested by theoretical considerations of Ca diffusion in small compartments such as the presynaptic terminal (Fogelson and Zucker, 1985; Neher, 1998; Simon and Llinás, 1985). Direct evidence for nanoscale coupling of Ca influx and downstream signaling mechanisms was shown in auditory hair cells (Roberts, 1993). The existence of nanoscale Ca subdomains within the microscale compartment physically provided by a single dendritic spine has recently been described as well. Yasuda et al. (2003) found that, while L-type VSCCs did not contribute an optically measurable amount of Ca to synaptically evoked signals in spines of CA1 pyramidal neurons, depression of R-type VSCC signaling following high-frequency spike trains required activation of L-type channels and downstream CaMKII- and cAMP-dependent signaling. The authors concluded that Ca influx through L-type channels must activate downstream effectors through Ca nanodomains that make little contribution to the bulk (microscale) Ca accumulation in the entire spine. In addition, studies have demonstrated that small-conductance Ca-activated potassium channels (SK channels) in hippocampal and amygdala dendritic spines contribute to shaping synaptic responses (see Figure 1) (Bloodgood and Sabatini, 2007; Faber et al., 2005; Ngo-Anh et al., 2005). Critically, in CA1 pyramidal neurons, SK channels are selectively activated by Ca influx through R-type VSCCs (Bloodgood and Sabatini, 2007), again indicating that a direct coupling between a Ca source and a downstream signaling pathway must occur via nanoscale domains within dendritic spines.

### Coincidence Detection and Dendritic Ca Spikes

Coincidence detection is a fundamental feature of neurons that allows signaling specificity in response to patterned synaptic inputs. Coincidence detection often takes the form of a nonlinear postsynaptic response, such as action potential initiation, following an appropriate spatiotemporal organization of afferent inputs. Several biophysical properties of Ca sources, including the voltage dependence of NMDARs and VSCCs, give rise to additional nonlinearities that may permit neuronal coincidence detection and play key roles in various neuronal processes including synaptic transmission and plasticity.

Paired recordings by Llinás and colleagues from the somata and dendrites of cerebellar Purkinje cells first revealed that complex spikes were mediated by dendritic Ca conductances (Llinás and Hess, 1976; Llinás and Nicholson, 1971). However, it was the advent of Ca imaging via fluorescent microscopy that allowed direct observation of dendritic Ca influx in both the cerebellum (Tank et al., 1988) and hippocampus (Regehr and Tank, 1990). Using ratiometric imaging of Fura-2, Regehr and Tank (1990) reported that high-frequency electrical stimulation of Schaeffer collateral inputs evoked a local supralinear Ca transient in the proximal apical dendrite of CA1 pyramidal neurons. The Ca response was regulated by both stimulation frequency and intensity, exhibiting a clear stepwise increase in amplitude

above a critical threshold (Regehr and Tank, 1990, 1992). The rise in Ca was spatially restricted to within  $\sim 150$   $\mu\text{m}$  of the site of synaptic activation and consisted of influx through both VSCCs (particularly L-types) and NMDARs. Similar results were found following synaptic stimulation of distal branches of the apical dendrite (Cai et al., 2004; Golding et al., 2002; Tsay et al., 2007; Wei et al., 2001), where both N- and T-type VSCCs may also contribute (Tsay et al., 2007). These all-or-none events, termed "Ca spikes," are thought to be analogous to the large-amplitude, broad dendritic spikes described electrophysiologically (Amitai et al., 1993; Golding et al., 1999; Remy and Spruston, 2007; Schwartzkroin and Slawsky, 1977; Stuart et al., 1997).

Using a combination of physiology, imaging, and computer simulations, Magee and colleagues have determined the spatio-temporal patterns of synaptic activation necessary to elicit dendritic Ca spikes. Asynchronous inputs delivered to radial oblique dendrites of CA1 pyramidal neurons produced somatic depolarizations that summed linearly and evoked little dendritic Ca influx. In contrast, highly temporally synchronized inputs exhibited supralinear summation of somatic voltage responses and produced a local Ca spike mediated by activation of VSCCs and NMDARs (see Figure 2) (Gasparini et al., 2004; Losonczy and Magee, 2006).

The voltage dependence of Ca influx through VSCCs and NMDARs provides a potential mechanism for the ability of neurons to perform coincidence detection. The biophysical properties of these Ca sources also permit a variety of other dendritic conductances to shape the amplitude and spatial spread of hippocampal dendritic Ca spikes. Voltage-dependent sodium channels are capable of promoting dendritic depolarization and thereby enhancing the amplitude of local Ca spikes (Gasparini et al., 2004; Losonczy and Magee, 2006). In addition, the magnitude, duration, and spatial extent of Ca spikes are regulated by potassium conductances, including A-type (Cai et al., 2004; Frick et al., 2003; Losonczy and Magee, 2006) and both large-conductance (Golding et al., 1999) and small-conductance (Cai et al., 2004) Ca-activated potassium channels. Furthermore, hyperpolarization-activated HCN1 channels constrain the amplitude of local Ca spikes by providing a tonic depolarizing drive that increases the resting inactivation of VSCCs involved in spike generation (Tsay et al., 2007).

Multiple studies have suggested a functional role for coincidence detection via dendritic Ca spikes, linking them to the generation of site-specific plasticity of hippocampal synaptic inputs. Theta-patterned or single high-frequency bursts of synaptic input via the perforant path are capable of evoking a local Ca spike in apical dendrites of CA1 pyramidal neurons. NMDAR and L-type VSCC blockade significantly reduced both the amplitude of the Ca spike and the expression of synapse-specific long-term potentiation (LTP), suggesting that local Ca spikes provide a mechanism for inducing synaptic plasticity in the absence of postsynaptic sodium-channel-mediated spike generation (Golding et al., 2002; Remy and Spruston, 2007).

A similar picture of dendritic Ca spike generation has emerged for cortical layer 5 pyramidal neurons. Yuste et al. (1994) described synaptically evoked peaks of Ca accumulation in localized regions of L5 pyramidal apical dendrites. Additional work showed that synaptic stimulation of the distal apical dendrite is

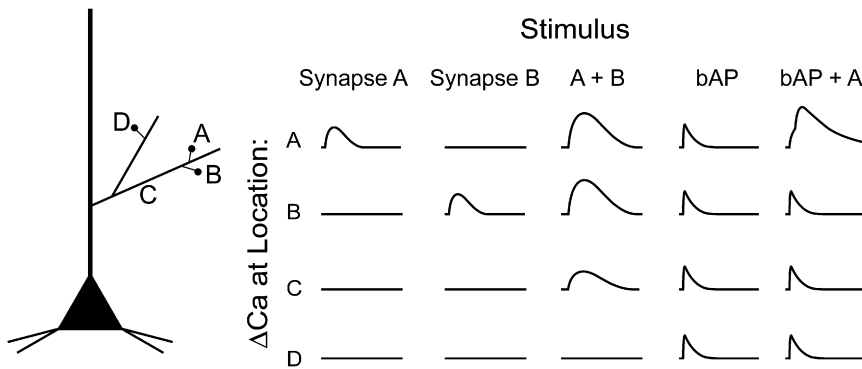


**Figure 2. Schematic Illustrating Some of the Features of Coincidence Detection via Dendritic Ca Signals**

The columns of traces illustrate hypothetical fluorescent signals from a Ca indicator measured at each location indicated on the pyramidal neuron on the left. A synaptic input to spine A (first column) or spine B (second column) produces a Ca transient limited to the active spine. Near-synchronous inputs to a cluster of spines (here showing only A and B, third column) produce a supralinear Ca signal within individual spines as well as a local Ca spike that extends into the neighboring dendrite (location C). Somatic generation of a back-propagating action potential (bAP, fourth column) produces more widespread Ca transients at all locations in the proximal dendritic arbor. Finally, pairing a bAP with synaptic input to location A (fifth column) produces a supralinear Ca signal within the active spine.

capable of evoking a local Ca spike limited to within  $\sim 50\text{--}150\ \mu\text{m}$  of the site of activation (Markram and Sakmann, 1994; Oakley et al., 2001; Schiller et al., 1997). These Ca spikes exhibit all-or-none generation and propagate poorly to the cell body. In contrast to the hippocampus, reports have consistently found that cortical apical dendritic Ca spikes are primarily dependent on VSCCs, with minimal contribution from NMDARs (Markram and Sakmann, 1994; Oakley et al., 2001), although Schiller et al. (1997) found that coactivation of both AMPARs and NMDARs was required to initiate the Ca transient.

Additional work has focused on the generation of so-called “NMDA spikes” in the basal dendrites of layer 5 pyramidal neurons. Schiller et al. (2000) showed that spatially clustered synaptic inputs could evoke large Ca transients in fine branches of the basal dendrites that were spatially restricted to the activated segment. Several groups have confirmed that these transients are primarily mediated by NMDAR activation (Major et al., 2008; Milojkovic et al., 2007; Schiller et al., 2000). In contrast to VSCC-mediated events, NMDA spikes are much more spatially restricted, limited to regions of glutamate release (Major et al., 2008). However, additional spread of the Ca signal beyond the site of synaptic activation can occur and appears to be mediated by subsequent engagement of VSCCs (Milojkovic et al., 2007). As in the hippocampus, these Ca spikes have been implicated in long-term changes in synaptic strength. Holthoff et al. (2004) found that a single stimulus applied to a basal dendrite could evoke an NMDA spike, producing Ca influx into both dendritic spines and neighboring shafts that resulted in site-specific long-term depression of synaptic inputs.

Synaptically evoked Ca nonlinearities can also occur in the absence of a clear “Ca spike.” In the striatum, near-synchronous activation of clustered synapses results in supralinear Ca influx within single dendritic spines that requires both NMDARs and L-type VSCCs (Carter et al., 2007). Furthermore, in CA1 pyramidal neurons, repetitive afferent stimulation in the stratum radiatum can evoke Ca waves in the thick apical dendrite that are mediated by activation of mGluRs and induce subsequent IP<sub>3</sub>-coupled Ca release from internal stores (Watanabe et al., 2006). In addition, pairing synaptic inputs via the perforant pathway and Schaeffer collaterals results in supralinear Ca accumulation in the apical dendrite and LTP of the Schaeffer inputs

(Dudman et al., 2007). Both the supralinear Ca influx and LTP require combined activation of NMDARs and perforant-path-mediated mGluR-IP<sub>3</sub> signaling.

Nonspike Ca nonlinearities are also observed in cerebellar Purkinje cells. In mature cerebellar Purkinje cells, dendritic spines lack functional NMDARs (Farrant and Cull-Candy, 1991). However, activation of afferent parallel fibers produces highly localized Ca influx within single spines due to AMPAR-mediated depolarization and subsequent activation of VSCCs (Eilers et al., 1995; Hartell, 1996). Moreover, activation of the climbing fiber produces complex spikes resulting in Ca influx via VSCCs throughout the proximal dendritic arbor (Ross and Werman, 1987). Pairing climbing fiber inputs with bursts of parallel fiber stimulation triggers supralinear Ca transients whose spatial extent is determined by the strength of parallel fiber input (Hartell, 1996; Wang et al., 2000). Strong stimulation produces a supralinear increase in Ca over large regions of dendrites that is dependent on VSCCs. In contrast, weaker stimulation can produce supralinear Ca influx limited to single dendritic spines. In this case, the amplified Ca signal is produced by release from internal stores following coactivation of IP<sub>3</sub> receptors by IP<sub>3</sub>, produced following parallel fiber activation of mGluRs, and Ca ions, accumulated following climbing fiber activation of VSCCs (Sarkisov and Wang, 2008; Wang et al., 2000). The synergistic action of Ca and IP<sub>3</sub> on Ca release from internal stores represents an additional biophysical mechanism for neuronal coincidence detection (Bezprozvanny et al., 1991; Finch et al., 1991). Furthermore, this mechanism is also subject to regulation, as large-conductance Ca-activated potassium channels act to reduce dendritic depolarization and VSCC activation, thereby limiting the spatial spread of the dendritic Ca signal (Rancz and Häusser, 2006).

As in the hippocampus and cortex, local Ca transients contribute to the induction of plasticity at parallel fiber-Purkinje cell synapses, resulting in the release of endocannabinoids that produce short-term reduction in synaptic efficacy and are necessary for long-term depression (LTD) of parallel fiber synapses (Brenowitz et al., 2006; Brown et al., 2003; Rancz and Häusser, 2006; Safa and Regehr, 2005). Furthermore, IP<sub>3</sub> receptor activation in the spine is necessary for mGluR-mediated LTD of parallel fiber synapses (Finch and Augustine, 1998; Inoue et al., 1998;

Miyata et al., 2000). Using myosin-Va knockouts lacking dendritic spine IP3 receptors, Miyata et al. (2000) found that mutant animals exhibited reduced Ca signaling in individual spines and failed to generate LTD of parallel fiber synapses, although LTD could be rescued by focal uncaging of IP3.

### Ca Signaling and Coincidence Detection during Suprathreshold Postsynaptic Activity

Dendritic Ca nonlinearities also play a role in signaling the occurrence of synaptic inputs that are sufficient to generate postsynaptic action potentials. In CA1 pyramidal neurons, somatic sodium-channel-mediated spikes generate widespread Ca signals by back propagating through the proximal dendritic arbor, producing sufficient depolarization to open VSCCs in both dendritic branches (Callaway and Ross, 1995; Christie et al., 1995; Jaffe et al., 1992; Spruston et al., 1995) and individual dendritic spines (see Figure 2) (Bloodgood and Sabatini, 2007; Hoogland and Saggau, 2004; Mainen et al., 1999; Sabatini and Svoboda, 2000; Yuste and Denk, 1995). Likewise, bAPs in cortical neurons generate widespread Ca signals in the dendrites and spines of layer 4 spiny stellate cells (Nevian and Sakmann, 2004) and pyramidal neurons in layers 2/3 (Nevian and Sakmann, 2006; Svoboda et al., 1997, 1999; Waters et al., 2003) and layer 5 (Helmchen et al., 1999; Kampa et al., 2006; Koester and Sakmann, 1998; Larkum et al., 1999b; Markram et al., 1995; Schiller et al., 1995; Yuste et al., 1994). bAP-generated Ca influx into dendrites and single spines also occurs in striatal medium spiny neurons (Carter and Sabatini, 2004) and in cerebellar Purkinje cells (Tank et al., 1988).

In most cases, bAP-evoked Ca signals exhibit greater magnitude in more proximal dendrites, decreasing with distance from the soma (Callaway and Ross, 1995; Christie et al., 1995; Jaffe et al., 1992; Svoboda et al., 1997, 1999). Moreover, in cortical layer 5 pyramidal neurons, there appears to be a “hot spot” or apical band ~500  $\mu\text{m}$  from the soma that exhibits significantly elevated Ca influx following spike generation (Larkum et al., 1999b; Yuste et al., 1994). The reasons for these spatial heterogeneities are not entirely resolved. Several reports indicate variability in the class and distribution of VSCCs in different compartments of dendrites and spines (Bloodgood and Sabatini, 2007; Christie et al., 1995; McKay et al., 2006; Sabatini and Svoboda, 2000; Westenbroek et al., 1990). However, variability in bAP-evoked Ca transients appears to be most related to the differential extent of sodium channel-mediated spike propagation through the dendritic arbor (Jaffe et al., 1992; Markram et al., 1995; Schiller et al., 1995; Waters et al., 2003). Gasparini et al. (2007) showed that local dendritic depolarization through a recording electrode is able to amplify both the bAP amplitude and the magnitude of Ca influx, while A-type potassium channels reduce the back propagation of both sodium spikes and resultant Ca influx in CA1 pyramidal neurons. Multiple groups have also shown that back propagation may be frequency dependent, with significant Ca influx occurring only following bursts of appropriately timed somatic spikes (Kampa et al., 2006; Larkum et al., 1999a; Waters et al., 2003).

In addition to generating a global Ca signal, bAPs contribute to neuronal coincidence detection by selectively boosting local dendritic Ca transients in response to synaptic activation (Fig-

ure 2). Pairing somatic action potentials with near-synchronous activation of synaptic inputs leads to supralinear Ca influx in the hippocampus, (Gasparini et al., 2007; Magee and Johnston, 1997; Yuste and Denk, 1995), cortex (Koester and Sakmann, 1998; Nevian and Sakmann, 2004, 2006; Schiller et al., 1998; Waters et al., 2003), striatum (Carter and Sabatini, 2004), and olfactory bulb (Egger et al., 2005). The Ca supralinearity is dependent on the activation of NMDARs (Carter and Sabatini, 2004; Schiller et al., 1998; Yuste et al., 1999) and extracellular magnesium concentration (Nevian and Sakmann, 2004), consistent with the view that the bAP provides sufficient depolarization to reduce Mg block, significantly increasing synaptic Ca influx. This model is supported by the finding that, in most cases, supralinear Ca influx occurs only when synaptic inputs precede bAP generation, as glutamate bound to NMDARs is required at the time of bAP-evoked depolarization (Koester and Sakmann, 1998; Nevian and Sakmann, 2004; Yuste et al., 1999). In contrast, sublinear Ca influx may occur when the bAP arrives first, although the mechanisms of this phenomenon are unclear (Koester and Sakmann, 1998; Nevian and Sakmann, 2004). Significant spine Ca influx was also observed with bAP-synaptic pairing in the presence of AMPAR antagonists, suggesting that pairing can evoke Ca influx at synapses that are “electrically silent” as one would expect for an NMDAR-dependent mechanism (Nevian and Sakmann, 2004).

Nevertheless, Ca nonlinearities following pairing of bAPs with synaptic inputs are not uniformly mediated by NMDAR dynamics. Nakamura et al. (1999) showed that bursts of spikes following strong synaptic stimulation could produce large Ca waves in CA1 apical dendrites that were mediated by synergistic actions of mGluR-coupled IP3 generation and bAP-associated Ca influx on IP3 receptors. In addition, bAPs lower the threshold for initiation of IP3-mediated Ca waves in CA1 apical dendrites following repetitive afferent stimulation (Watanabe et al., 2006), and trains of bAPs can serve to prime internal Ca stores for subsequent release (Hong and Ross, 2007).

As with dendritic Ca spikes, the supralinear increases in Ca following bAP-synaptic pairing have been linked with the induction of spike-timing-dependent plasticity (STDP), where repetitive pairing of synaptic activity with bAP generation can produce long-term site-specific changes in synaptic efficacy (Dan and Poo, 2004; Kampa et al., 2007; Magee and Johnston, 1997; Markram et al., 1997). In most cases, when synaptic activation occurs before postsynaptic spiking (pre-post), synapses exhibit LTP, while the reverse timing (post-pre) yields LTD. Multiple studies have linked the supralinear Ca influx through NMDARs seen when synaptic stimuli preceded bAPs to the generation of LTP (Bender et al., 2006; Magee and Johnston, 1997; Nevian and Sakmann, 2006). In contrast, the relatively reduced Ca influx that occurs when bAPs precede the synaptic stimulus, particularly when coupled with synaptic activation of mGluRs, leads to PLC-dependent synthesis of endocannabinoids and generation of LTD (Bender et al., 2006; Nevian and Sakmann, 2006; Safo and Regehr, 2005; Sjöström et al., 2008). Nevertheless, the specific connection between Ca influx and plasticity remains unclear. Some authors have suggested that the direction of plasticity is determined by the degree of Ca elevation (Cormier et al., 2001; Ismailov et al., 2004). However, Nevian and Sakmann

(2006) found that both LTP and LTD protocols could produce similar Ca transients, and the absolute magnitude of Ca influx was not correlated with the direction of synaptic plasticity. Furthermore, the window for spike-timing-dependent LTP is ~5–30 ms, an interval considerably shorter than both the dissociation time for glutamate from NMDARs (Clements et al., 1992; Vicini et al., 1998) and the observed window of supralinear Ca influx (Koester and Sakmann, 1998; Nevian and Sakmann, 2006). Similarly, the mechanism for LTD also remains unclear, with other studies suggesting the involvement of L-type Ca channels (Bi and Poo, 1998) or Ca release from internal stores (Nishiyama et al., 2000).

## Section II. Monitoring and Quantifying Ca Signals in Neuronal Compartments

In this next section, we will discuss the interpretation of fluorescence transients collected in the course of Ca imaging experiments, focusing on two main goals. First, we describe a simple but quantitative framework that can be used to interpret fluorescence transients from Ca indicators and highlight basic facts about Ca imaging that are often overlooked. These concepts are based on the extensive treatment of intracellular Ca buffering by Neher and colleagues (Neher and Augustine, 1992; Zhou and Neher, 1993). Second, we differentiate between the conditions necessary to accurately measure changes in the concentration of intracellular calcium ([Ca]) following a stimulus versus those needed to determine the relative contributions of multiple Ca sources to stimulus-evoked Ca transients.

Intracellular Ca reversibly binds to endogenous molecules such as Ca-binding proteins (e.g., calbindin, parvalbumin, calmodulin) (Schwaller et al., 2002). In addition, Ca binds to experimentally introduced molecules such as synthetic Ca buffers (e.g., EGTA, BAPTA, Fura-2, Fluo-4) and genetically encoded Ca indicators (e.g., Chameleon, GCAMP, TN-XL). Fluorescent Ca indicators are molecules that undergo a conformational change on binding Ca that alters either their fluorescence absorption or emission properties. Therefore, measuring intracellular [Ca] requires the introduction of a Ca-binding molecule and necessarily perturbs the dynamics of Ca transients compared to the natural state. Understanding this perturbation is critical for accurate interpretation of Ca-related fluorescent signals, and throughout this section, we develop and highlight five key points regarding the experimental use of fluorescent Ca indicators.

### Ca and Fluorescent Indicators Are in Equilibrium

The interaction between Ca and Ca buffer is described by the second-order kinetic equation:



where [Ca], [B], and [BCa] represent the concentrations of free Ca, free buffer, and Ca-bound buffer, respectively. For many synthetic Ca indicators, the forward rate constant ( $k_{on}$ ) is nearly diffusion limited, whereas the reverse rate constant ( $k_{off}$ ) varies and determines the equilibrium or dissociation constant  $K_D$  ( $K_D = k_{off}/k_{on}$ ). For typical experiments, reaction (1) locally reaches

equilibrium within ~100  $\mu$ s, in which time Ca diffuses far less than 1  $\mu$ m (although longer equilibration times may occur in the presence of very high affinity indicators, particularly those that bind multiple divalent ions, or when endogenous buffering is high [Kao and Tsien, 1988; Naraghi, 1997; Sabatini and Regehr, 1998]). Thus, considering the typical data acquisition rates and spatial resolutions of Ca imaging experiments, [Ca] and [B] are assumed to be in local equilibrium. That is:

$$K_D = \frac{[Ca][B]}{[BCa]} \quad (2)$$

As the total concentration of buffer ( $B_T$ ) is constant, with  $B_T = [B] + [BCa]$ , Equation 2 can be rewritten as:

$$[BCa] = B_T \frac{[Ca]}{[Ca] + K_D} \quad (3)$$

Equation 3 can be used to plot [BCa] as a function of [Ca], yielding binding curves typical of two particle interactions (Figure 3A). For many modern, high dynamic range fluorescence Ca indicators such as Fluo-4 and Fluo-5, free indicator (i.e., not bound to Ca) is nearly nonfluorescent. Therefore, experimentally measured fluorescence (F) is primarily contributed by [BCa], and we can assume that  $F = \alpha[BCa]$ . The value of the constant  $\alpha$  depends on the properties of the indicator (e.g., cross-section, quantum efficiency, excitation and emission spectra), microscope (e.g., illumination power, numerical aperture of the objective, detectors used to collect light), and sample (e.g., size of the imaged structure, absorptive properties of the tissue). Note that this direct relationship between [BCa] and fluorescence does not hold when using indicators such as Mg-green, which substantially bind divalent ions other than Ca, or Fura-2, which possesses more than one Ca-binding site and also exhibits fluorescence in the Ca-unbound state (Henke et al., 1996). Furthermore, the relationship breaks down when using imaging modalities such as whole-field fluorescence, in which background fluorescence (e.g., tissue autofluorescence) is not negligible, particularly in small (and therefore dim) structures such as spines and dendrites. The relative lack of tissue autofluorescence is a major advantage of measuring spine and dendrite fluorescence with two-photon laser-scanning microscopy.

Point 1: The measured fluorescence from a Ca indicator is proportional to [BCa] (with possible contributions from [B] and autofluorescence) but not to [Ca].

### Buffer Capacity Determines the Response of Indicator to Changes in [Ca]

In Figure 3A, the relationships between [BCa] and [Ca] are plotted for two buffers with different affinities ( $K_D = 0.2$  or  $1.0 \mu$ M) and for multiple concentrations of total buffer ( $B_T = 75, 150,$  or  $300 \mu$ M). On each curve, we have plotted the point representing a resting spine ( $[Ca]_{rest} = 0.1 \mu$ M) with a square. Note that  $[Ca]_{rest}$  is the value at which Ca influx and efflux are balanced and is independent of changes in Ca buffer. Subsequent points, plotted as circles, represent changes from rest due to a series of action

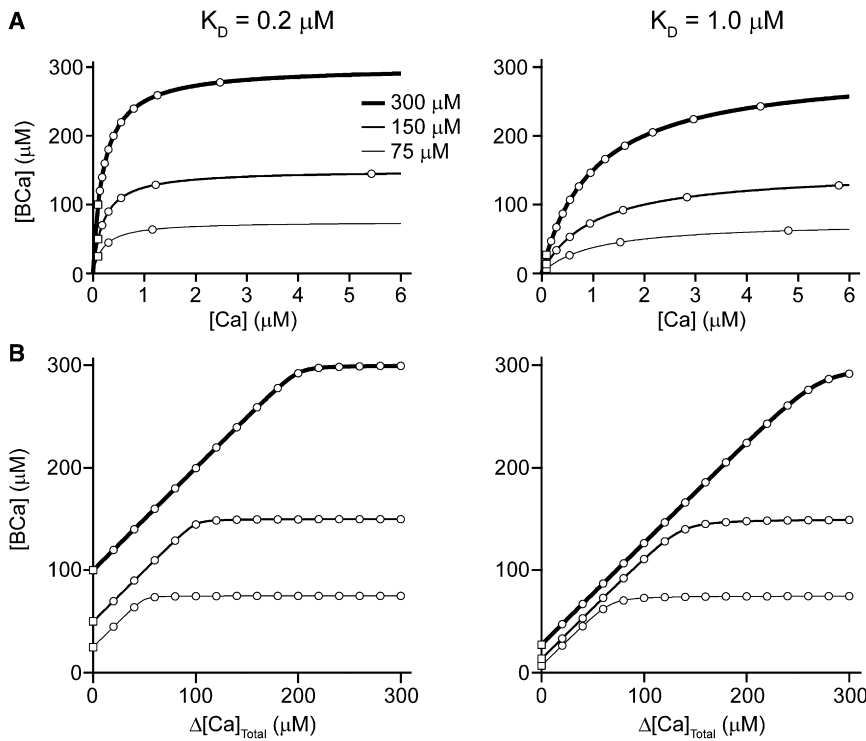


**Figure 3. The Relationships between Ca-Bound Indicator ([BCa]) and Free Ca ([Ca]) or Total Ca ( $Ca_T$ )**

(A) The relationship between [BCa] and [Ca] is plotted for a buffer with  $K_D = 0.2 \mu\text{M}$  (left) or  $K_D = 1.0 \mu\text{M}$  (right). Curves have been calculated for a total buffer concentration ( $B_T = [\text{BCa}] + [\text{B}]$ ) of either 75, 150, or  $300 \mu\text{M}$  (see Equation 3). The values for [BCa] corresponding to resting [Ca] (squares) or [Ca] following a series of APs (circles) are plotted. Values for resting [Ca] as well as the total Ca influx per AP ( $\Delta Ca_T = 20 \mu\text{M}$ ) were based on studies of hippocampal pyramidal neurons. As [Ca] increases, the buffer becomes saturated, and the slope of each curve becomes dramatically sublinear. Furthermore, because of buffer saturation, the rise in [Ca] for each AP becomes progressively larger.

(B) The relationship between [BCa] and total Ca influx above rest ( $\Delta Ca_T$ ) is plotted (see Equation 9) using the same values for  $K_D$  and  $B_T$  as in (A). In contrast to (A), the curves have a large linear region with a slope  $\sim 1.0$  (see Equation 10). The curves become sublinear only following near-complete saturation of the buffer.

potentials (APs), each of which contributes  $20 \mu\text{M}$  of total calcium ( $Ca_T = [\text{Ca}] + [\text{BCa}]$ ) to the spine. For these examples, values are chosen to match those measured in apical spines of hippocampal CA1 pyramidal neurons (Sabatini et al., 2002) and may vary for other cell classes.

With each subsequent AP, the change in [BCa] ( $\Delta[\text{BCa}]$ ) becomes progressively smaller compared to the change in [Ca] ( $\Delta[\text{Ca}]$ ). The relationship between  $\Delta[\text{BCa}]$  and  $\Delta[\text{Ca}]$  is described quantitatively by the buffer capacity,  $\kappa_B$ , defined as the incremental change in [BCa] for an incremental change in free [Ca] (Neher and Augustine, 1992):

$$\kappa_B = \frac{\partial[\text{BCa}]}{\partial[\text{Ca}]} \approx \frac{\Delta[\text{BCa}]}{\Delta[\text{Ca}]} \quad (4)$$

This equation, in the differential form, gives the slope of the curves in Figure 3A. The nonlinearity of each curve indicates that  $\kappa_B$  is not constant but decreases as [Ca] increases. Intuitively, at higher [Ca], a greater fraction of the total buffer is bound and less is available to sequester further increases in [Ca]. The differential form of Equation 4 defines  $\kappa_B$  for an infinitesimal change in [Ca] ( $\delta[\text{Ca}]$ ). However, most experiments involve detecting larger changes in [Ca] ( $\Delta[\text{Ca}]$ ). Therefore,  $\kappa_B$  can be approximated by combining the difference form of Equation 4 with Equation 3 to yield:

$$\kappa_B = \frac{B_T K_D}{(K_D + [\text{Ca}]_{\text{rest}})(K_D + [\text{Ca}]_{\text{rest}} + \Delta[\text{Ca}])} \quad (5)$$

Equation 5 demonstrates that, as either the total buffer concentration or its Ca affinity increases, the buffer capacity increases.

The utility of treating  $\kappa_B$  quantitatively is that its value predicts features of stimulus-evoked Ca transients and corresponding fluorescence. For example, if a stimulus such as a single AP increases  $Ca_T$  in a spine by  $\Delta Ca_T$  ( $20 \mu\text{M}$  in Figure 3), the corresponding  $\Delta[\text{Ca}]$  is given by:

$$\Delta[\text{Ca}] = \frac{\Delta Ca_T}{1 + \kappa_T} \quad (6)$$

Equation 6 is derived from Equation 4 using  $\Delta Ca_T = \Delta[\text{Ca}] + \Delta[\text{BCa}]$  and replacing  $\kappa_B$  with  $\kappa_T$ , the sum of the individual buffer capacities for all endogenous and exogenous Ca-binding molecules. Thus,  $\Delta[\text{Ca}]$ , the stimulus-evoked change in free Ca, scales inversely with  $\kappa_T$  such that, at higher buffer capacities, less Ca remains free for a given  $\Delta Ca_T$ .

Point 2: The change in free-Ca concentration ( $\Delta[\text{Ca}]$ ) that occurs following a change in total Ca concentration ( $\Delta Ca_T$ ) is directly determined by the total buffer capacity of the dendritic compartment.

### Determinants of the Linearity of Fluorescence Measurements

Several groups have used equilibrium equations to derive  $\Delta[\text{Ca}]$  from stimulus-evoked changes in fluorescence (Grynkiewicz et al., 1985; Maravall et al., 2000). While this approach has been used successfully, it requires knowledge or approximation of indicator fluorescence in the presence of both zero and saturating [Ca], parameters that can be difficult to determine within dendrites and spines of neurons in a brain slice. One potential simplifying solution is to assume, under specific conditions, a

linear relationship between  $\Delta[\text{Ca}]$  and  $\Delta[\text{BCa}]$  (and thus fluorescence). When a buffer is present at high concentrations and  $[\text{Ca}] \ll K_D$ , Equations 4 and 5 can be approximated as:

$$[\text{BCa}] = \kappa_B [\text{Ca}] \quad (7)$$

$$\kappa_B = \frac{B_T}{K_D} \quad (8)$$

Under these conditions, there is a direct proportionality linking  $[\text{Ca}]$  and  $[\text{BCa}]$  (and, by extension, fluorescence), and the indicator is said to be “in a linear range.” However, Equations 7 and 8 will always underestimate actual  $[\text{Ca}]$ , and the range over which they can be used with acceptable errors is remarkably small. Consider the situation in which the buffer is half occupied (i.e.,  $[\text{BCa}] = [\text{B}] = B_T/2$ ). Equilibrium (see Equation 3) dictates that  $[\text{Ca}] = K_D$ . However, Equations 7 and 8 predict that  $[\text{Ca}] = K_D/2$ —an error of 100%! In fact, to assume linearity and underestimate true  $[\text{Ca}]$  by less than 25%,  $[\text{Ca}]$  must be kept below  $K_D/4$ .

Point 3: In order to consider the relationship between  $[\text{BCa}]$  and  $[\text{Ca}]$  to be linear and thus allow Equations 7 and 8 to provide a reasonable approximation, free  $[\text{Ca}]$  must remain several-fold smaller than the  $K_D$  of the indicator.

In many studies, the goal is to quantify the relative contributions of various Ca sources to a stimulus-evoked transient rather than to determine the absolute  $[\text{Ca}]$ . For example, what fractions of synaptically evoked Ca transients in spines are contributed by NMDA-type glutamate receptors (NMDARs) versus voltage-sensitive Ca channels (VSCCs)? For these studies, it is a mistake to use calculations of  $\Delta[\text{Ca}]$  to compare the Ca influx under different conditions.

Instead, the total stimulus-evoked Ca influx ( $\Delta\text{Ca}_T$ ) can be measured directly from the change in fluorescence (i.e.,  $\Delta[\text{BCa}]$ ), a relationship that is surprisingly insensitive to changes in buffer capacity over a wide range. This result can be seen in Figure 3B, where  $[\text{BCa}]$  is plotted as a function of  $\text{Ca}_T$  added above rest using the following:

$$[\text{BCa}] = 1/2 \left[ (\text{Ca}_T + B_T + K_D) - \sqrt{(\text{Ca}_T + B_T + K_D)^2 - 4(B_T \cdot \text{Ca}_T)} \right] \quad (9)$$

Equation 9 is derived from Equation 3 using  $\text{Ca}_T = [\text{Ca}] + [\text{BCa}]$  and solving for  $[\text{BCa}]$ . As in Figure 3A, points are plotted as circles for a series of APs, where each AP adds 20  $\mu\text{M}$  total Ca to the spine. Note that values for  $[\text{BCa}]$  at  $\Delta\text{Ca}_T = 0$  represent resting concentrations of bound buffer in the spine. For a variety of indicator concentrations and affinities, the relationship between  $[\text{BCa}]$  and  $\text{Ca}_T$  has a linear region with a slope of  $\sim 1$  (i.e.,  $\Delta[\text{BCa}]$  is approximately equal to  $\Delta\text{Ca}_T$ ). This result occurs in ranges over which the evoked change in free  $[\text{Ca}]$  per AP is already substantially nonlinear (compare with Figure 3A) and can be explained by considering buffer capacity in terms of total Ca rather than free Ca. Combining Equations 4 and 6 yields:

$$\Delta[\text{BCa}] = \Delta\text{Ca}_T \frac{\kappa_B}{1 + \kappa_T} \quad (10)$$

In the typical case in which the experimenter has added sufficient indicator to dominate the buffer capacity of the cell, whose contribution can be ignored (i.e.,  $\kappa_T \approx \kappa_B \gg 1$ ),  $\Delta[\text{BCa}]$  can be used as an estimate for  $\Delta\text{Ca}_T$  to within 10% error until the  $\kappa_B$  drops to a value of  $\sim 10$ . This conclusion holds when the endogenous buffer capacity of the neuron is low, as in the thin dendrites and spines of pyramidal neurons (Noguchi et al., 2005; Sabatini et al., 2002). However, buffer domination may be more challenging in interneurons and Purkinje cells that have higher endogenous Ca-binding capacities, presumably due to higher concentration of Ca-binding proteins (Fierro and Llano, 1996; Lee et al., 2000).

Point 4. Stimulus-evoked changes in  $[\text{BCa}]$ , as estimated by changes in fluorescence, are linearly proportional to the total Ca influx,  $\Delta\text{Ca}_T$ , over a broad range. This linearity is preserved over a range in which a large fraction of the buffer is bound to Ca and in which the relationship between  $[\text{BCa}]$  and  $[\text{Ca}]$  is clearly nonlinear.

### Kinetic and Diffusional Effects of Ca Indicators

Thus far, we have considered the effects of Ca-binding molecules on the magnitude of changes in free and total Ca. We now briefly outline the effects of indicator on the kinetics and spatial spread of stimulus-evoked changes in  $[\text{Ca}]$  within spines and dendrites.

In response to a rapid rise in  $\text{Ca}_T$  within a small compartment, as occurs following an AP,  $[\text{Ca}]$  rises quickly and then returns to resting levels via various Ca extrusion and sequestration mechanisms with a time course that can be well-approximated by a single exponential with decay time constant  $\tau$  (Sabatini et al., 2002; Scheuss et al., 2006; Yuste and Denk, 1995). The presence of Ca buffers slows the clearance of Ca according to:

$$\tau = \frac{(1 + \kappa_T)}{\gamma} \quad (11)$$

where  $\gamma$  is the rate of Ca clearance from the compartment and  $\kappa_T$  is the sum of the individual buffer capacities for all intracellular Ca-binding molecules. Thus, an increase in buffer capacity, as occurs following the introduction of fluorescent Ca indicator, slows the decay of intracellular Ca levels. Notably, this slowing occurs by the same amount that the peak magnitude is reduced (see Equation 6). Thus, the integral of the Ca transient is less sensitive than the peak magnitude to variability in buffer capacity. Importantly, investigators measuring changes in Ca via fluorescent indicators must remain aware that the kinetics of the measured response are typically a considerably filtered version of the unperturbed signal.

Intracellular buffers also markedly perturb the spatial diffusion of Ca molecules through the cytoplasm. Endogenous Ca buffers can be grouped by their diffusion properties as either mobile or immobile, whereas experimentally introduced indicators are generally highly mobile. Intracellular movement of Ca can be characterized by an effective diffusion coefficient,  $D_{\text{eff}}$ , that is dependent on the diffusion coefficients of free Ca ( $D_{\text{Ca}}$ ) and Ca bound to both mobile endogenous buffers ( $D_M$ ) and indicator ( $D_{\text{Dye}}$ ), as well as the buffer capacities of both buffers:



$$D_{\text{eff}} = \frac{(D_{\text{Ca}} + D_M \cdot \kappa_M + D_{\text{Dye}} \cdot \kappa_{\text{Dye}})}{(1 + \kappa_M + \kappa_I + \kappa_{\text{Dye}})} \quad (12)$$

where  $\kappa_M$  and  $\kappa_I$  designate the buffer capacities of the mobile and immobile endogenous buffers, respectively. The diffusion coefficient of the immobile buffer is set to zero and hence does not appear in the numerator. In most cases, the mobility of experimentally introduced Ca indicators is significantly larger than that of endogenous buffers (Gabso et al., 1997; Hernandez-Cruz et al., 1990), significantly increasing the distance over which Ca molecules travel in the cytoplasm. This result has the consequence of potentially breaking down the compartmentalization of microdomain signaling normally established by various Ca-binding molecules (Goldberg et al., 2003; Soler-Llavina and Sabatini, 2006). Thus, experiments concerned with measuring spatially restricted Ca signaling must pay particular concern to the actions of introduced indicators.

Point 5: The introduction of Ca indicators can significantly decrease the amplitude, prolong the time course, and extend the spatial spread of intracellular  $\Delta[\text{Ca}]$  in comparison to the unperturbed state. These consequences may significantly disrupt normal Ca signaling.

### Concluding Thoughts

In this review, we have discussed the practical considerations regarding the measurement and interpretation of Ca-sensitive fluorescent imaging data and highlighted several examples of how optical studies have expanded our knowledge of dendritic Ca signaling. A large body of evidence now exists showing that, despite the diversity of spatiotemporally overlapping Ca sources, signaling can occur with great specificity due to both compartmentally restricted Ca transients and nonlinear summation in response to precise patterns of neuronal activity. Nevertheless, while the last few decades have witnessed enormous strides in our understanding, a number of open questions remain to be explored and answered.

First, the consequences of perturbed Ca diffusion due to the highly mobile fluorescent indicators on normal Ca signaling are almost certainly underappreciated. In particular, the existence and function of compartmentalized Ca signaling at the microdomain scale remains a fascinating but elusive subject, largely due to the difficulty in imaging Ca transients with minimal disruption of the diffusional restrictions that support these signaling environments. In addition, the characterization of dendritic Ca spikes as “all-or-none” may understate the importance of more subtle graded changes in  $[\text{Ca}]$  that are masked by the saturation of moderate to high affinity indicators. The continued development of lower-affinity indicators that preserve a measurable fluorescent signal will greatly facilitate additional insights into the fine details of dendritic Ca handling.

Second, the functional role of Ca molecules as second messengers in dendritic biochemical signaling remains unclear. A variety of Ca-sensitive downstream molecules, such as calmodulin, are known to couple rises in Ca concentration to subsequent changes in synaptic and cell function (Colbran and Brown, 2004). However, in most cases the precise mechanisms

linking changes in  $[\text{Ca}]$  to functional consequences have not been established. The similarities between Ca nonlinearities and STDP following bAP-synaptic pairing are highly suggestive of a causal connection. However, clear differences between these two phenomena highlight the need for continued investigation of the exact role played by Ca in cell signaling.

Finally, several studies demonstrate the ability of dendritic Ca transients to herald near-synchronous and spatially clustered synaptic activation. However, most of this evidence has been acquired in brain slices using forms of synaptic activation that may not closely resemble in vivo conditions. The intact brain is awash with robust and behaviorally context-specific patterns of synchronous neuronal activity (Buzsaki and Draguhn, 2004; Llinás and Steriade, 2006; Stevens and Zador, 1998). Moreover, neurons in vivo are influenced by both excitatory and inhibitory synaptic connections as well as state-dependent actions of myriad neuromodulators. One of the major hurdles in experimental neuroscience is the need to understand how these global patterns of network activity map onto the specific activation of individual synapses, thus making use of the varied and dynamic mechanisms of dendritic Ca signaling.

### ACKNOWLEDGMENTS

The authors thank members of the Sabatini Lab and J.A. Cardin for helpful comments during the preparation of this manuscript. M.J.H. is supported by a Postdoctoral Research Fellowship from the Parkinson's Disease Foundation.

### REFERENCES

- Amitai, Y., Friedman, A., Connors, B.W., and Gutnick, M.J. (1993). Regenerative activity in apical dendrites of pyramidal cells in neocortex. *Cereb. Cortex* 3, 26–38.
- Bender, V.A., Bender, K.J., Brasier, D.J., and Feldman, D.E. (2006). Two coincidence detectors for spike timing-dependent plasticity in somatosensory cortex. *J. Neurosci.* 26, 4166–4177.
- Bezprozvanny, I., Watras, J., and Ehrlich, B.E. (1991). Bell-shaped calcium-response curves of  $\text{Ins}(1,4,5)\text{P}_3$ - and calcium-gated channels from endoplasmic reticulum of cerebellum. *Nature* 351, 751–754.
- Bi, G.Q., and Poo, M.M. (1998). Synaptic modifications in cultured hippocampal neurons: dependence on spike timing, synaptic strength, and postsynaptic cell type. *J. Neurosci.* 18, 10464–10472.
- Bloodgood, B.L., and Sabatini, B.L. (2007). Nonlinear regulation of unitary synaptic signals by  $\text{CaV}(2.3)$  voltage-sensitive calcium channels located in dendritic spines. *Neuron* 53, 249–260.
- Brenowitz, S.D., Best, A.R., and Regehr, W.G. (2006). Sustained elevation of dendritic calcium evokes widespread endocannabinoid release and suppression of synapses onto cerebellar Purkinje cells. *J. Neurosci.* 26, 6841–6850.
- Brown, S.P., Brenowitz, S.D., and Regehr, W.G. (2003). Brief presynaptic bursts evoke synapse-specific retrograde inhibition mediated by endogenous cannabinoids. *Nat. Neurosci.* 6, 1048–1057.
- Burnashev, N., Monyer, H., Seeburg, P.H., and Sakmann, B. (1992). Divalent ion permeability of AMPA receptor channels is dominated by the edited form of a single subunit. *Neuron* 8, 189–198.
- Buzsaki, G., and Draguhn, A. (2004). Neuronal oscillations in cortical networks. *Science* 304, 1926–1929.
- Cai, X., Liang, C.W., Muralidharan, S., Muralidharan, S., Kao, J.P., Tang, C.M., and Thompson, S.M. (2004). Unique roles of SK and Kv4.2 potassium channels in dendritic integration. *Neuron* 44, 351–364.

- Callaway, J.C., and Ross, W.N. (1995). Frequency-dependent propagation of sodium action potentials in dendrites of hippocampal CA1 pyramidal neurons. *J. Neurophysiol.* *74*, 1395–1403.
- Carter, A.G., and Sabatini, B.L. (2004). State-dependent calcium signaling in dendritic spines of striatal medium spiny neurons. *Neuron* *44*, 483–493.
- Carter, A.G., Soler-Llavina, G.J., and Sabatini, B.L. (2007). Timing and location of synaptic inputs determine modes of subthreshold integration in striatal medium spiny neurons. *J. Neurosci.* *27*, 8967–8977.
- Christie, B.R., Eliot, L.S., Ito, K., Miyakawa, H., and Johnston, D. (1995). Different Ca<sup>2+</sup> channels in soma and dendrites of hippocampal pyramidal neurons mediate spike-induced Ca<sup>2+</sup> influx. *J. Neurophysiol.* *73*, 2553–2557.
- Clements, J.D., Lester, R.A., Tong, G., Jahr, C.E., and Westbrook, G.L. (1992). The time course of glutamate in the synaptic cleft. *Science* *258*, 1498–1501.
- Colbran, R.J., and Brown, A.M. (2004). Calcium/calmodulin-dependent protein kinase II and synaptic plasticity. *Curr. Opin. Neurobiol.* *14*, 318–327.
- Cormier, R.J., Greenwood, A.C., and Connor, J.A. (2001). Bidirectional synaptic plasticity correlated with the magnitude of dendritic calcium transients above a threshold. *J. Neurophysiol.* *85*, 399–406.
- Cowan, W.M., Sudhof, T.C., and Stevens, C.F., eds. (2001). *Synapses* (Baltimore, MD: The Johns Hopkins University Press).
- Cull-Candy, S., Kelly, L., and Farrant, M. (2006). Regulation of Ca<sup>2+</sup>-permeable AMPA receptors: synaptic plasticity and beyond. *Curr. Opin. Neurobiol.* *16*, 288–297.
- Dan, Y., and Poo, M.M. (2004). Spike timing-dependent plasticity of neural circuits. *Neuron* *44*, 23–30.
- Day, M., Wang, Z., Ding, J., An, X., Ingham, C.A., Shering, A.F., Wokosin, D., Ilijic, E., Sun, Z., Sampson, A.R., et al. (2006). Selective elimination of glutamatergic synapses on striatopallidal neurons in Parkinson disease models. *Nat. Neurosci.* *9*, 251–259.
- Denk, W., Sugimori, M., and Llinás, R. (1995). Two types of calcium response limited to single spines in cerebellar Purkinje cells. *Proc. Natl. Acad. Sci. USA* *92*, 8279–8282.
- Doering, C.J., and Zamponi, G.W. (2003). Molecular pharmacology of high voltage-activated calcium channels. *J. Bioenerg. Biomembr.* *35*, 491–505.
- Dudman, J.T., Tsay, D., and Siegelbaum, S.A. (2007). A role for synaptic inputs at distal dendrites: instructive signals for hippocampal long-term plasticity. *Neuron* *56*, 866–879.
- Egger, V., Svoboda, K., and Mainen, Z.F. (2005). Dendrodendritic synaptic signals in olfactory bulb granule cells: local spine boost and global low-threshold spike. *J. Neurosci.* *25*, 3521–3530.
- Eilers, J., Augustine, G.J., and Konnerth, A. (1995). Subthreshold synaptic Ca<sup>2+</sup> signalling in fine dendrites and spines of cerebellar Purkinje neurons. *Nature* *373*, 155–158.
- Emptage, N., Bliss, T.V., and Fine, A. (1999). Single synaptic events evoke NMDA receptor-mediated release of calcium from internal stores in hippocampal dendritic spines. *Neuron* *22*, 115–124.
- Faber, E.S., Delaney, A.J., and Sah, P. (2005). SK channels regulate excitatory synaptic transmission and plasticity in the lateral amygdala. *Nat. Neurosci.* *8*, 635–641.
- Farrant, M., and Cull-Candy, S.G. (1991). Excitatory amino acid receptor-channels in Purkinje cells in thin cerebellar slices. *Proc. Biol. Sci.* *244*, 179–184.
- Fierro, L., and Llano, I. (1996). High endogenous calcium buffering in Purkinje cells from rat cerebellar slices. *J. Physiol.* *496*, 617–625.
- Finch, E.A., and Augustine, G.J. (1998). Local calcium signalling by inositol 1,4,5-trisphosphate in Purkinje cell dendrites. *Nature* *396*, 753–756.
- Finch, E.A., Turner, T.J., and Goldin, S.M. (1991). Calcium as a coagonist of inositol 1,4,5-trisphosphate-induced calcium release. *Science* *252*, 443–446.
- Fogelson, A.L., and Zucker, R.S. (1985). Presynaptic calcium diffusion from various arrays of single channels. Implications for transmitter release and synaptic facilitation. *Biophys. J.* *48*, 1003–1017.
- Frick, A., Magee, J., Koester, H.J., Migliore, M., and Johnston, D. (2003). Normalization of Ca<sup>2+</sup> signals by small oblique dendrites of CA1 pyramidal neurons. *J. Neurosci.* *23*, 3243–3250.
- Gabso, M., Neher, E., and Spira, M.E. (1997). Low mobility of the Ca<sup>2+</sup> buffers in axons of cultured *Aplysia* neurons. *Neuron* *18*, 473–481.
- Gasparini, S., Migliore, M., and Magee, J.C. (2004). On the initiation and propagation of dendritic spikes in CA1 pyramidal neurons. *J. Neurosci.* *24*, 11046–11056.
- Gasparini, S., Losonczy, A., Chen, X., Johnston, D., and Magee, J.C. (2007). Associative pairing enhances action potential back-propagation in radial oblique branches of CA1 pyramidal neurons. *J. Physiol.* *580*, 787–800.
- Goldberg, J.H., Tamas, G., Aronov, D., and Yuste, R. (2003). Calcium microdomains in aspiny dendrites. *Neuron* *40*, 807–821.
- Golding, N.L., Jung, H.Y., Mickus, T., and Spruston, N. (1999). Dendritic calcium spike initiation and repolarization are controlled by distinct potassium channel subtypes in CA1 pyramidal neurons. *J. Neurosci.* *19*, 8789–8798.
- Golding, N.L., Staff, N.P., and Spruston, N. (2002). Dendritic spikes as a mechanism for cooperative long-term potentiation. *Nature* *418*, 326–331.
- Grynkiewicz, G., Poenie, M., and Tsien, R.Y. (1985). A new generation of Ca<sup>2+</sup> indicators with greatly improved fluorescence properties. *J. Biol. Chem.* *260*, 3440–3450.
- Hartell, N.A. (1996). Strong activation of parallel fibers produces localized calcium transients and a form of LTD that spreads to distant synapses. *Neuron* *16*, 601–610.
- Helmchen, F., Svoboda, K., Denk, W., and Tank, D.W. (1999). In vivo dendritic calcium dynamics in deep-layer cortical pyramidal neurons. *Nat. Neurosci.* *2*, 989–996.
- Henke, W., Cetinsoy, C., Jung, K., and Loening, S. (1996). Non-hyperbolic calcium calibration curve of Fura-2: implications for the reliability of quantitative Ca<sup>2+</sup> measurements. *Cell Calcium* *20*, 287–292.
- Hernandez-Cruz, A., Sala, F., and Adams, P.R. (1990). Subcellular calcium transients visualized by confocal microscopy in a voltage-clamped vertebrate neuron. *Science* *247*, 858–862.
- Hille, B. (2001). *Ion Channels of Excitable Membranes*, Third Edition (Sunderland, MA: Sinauer Associates).
- Holthoff, K., Kovalchuk, Y., Yuste, R., and Konnerth, A. (2004). Single-shock LTD by local dendritic spikes in pyramidal neurons of mouse visual cortex. *J. Physiol.* *560*, 27–36.
- Hong, M., and Ross, W.N. (2007). Priming of intracellular calcium stores in rat CA1 pyramidal neurons. *J. Physiol.* *584*, 75–87.
- Hoogland, T.M., and Saggau, P. (2004). Facilitation of L-type Ca<sup>2+</sup> channels in dendritic spines by activation of beta<sub>2</sub> adrenergic receptors. *J. Neurosci.* *24*, 8416–8427.
- Inoue, T., Kato, K., Kohda, K., and Mikoshiba, K. (1998). Type 1 inositol 1,4,5-trisphosphate receptor is required for induction of long-term depression in cerebellar Purkinje neurons. *J. Neurosci.* *18*, 5366–5373.
- Ismailov, I., Kalikoulov, D., Inoue, T., and Friedlander, M.J. (2004). The kinetic profile of intracellular calcium predicts long-term potentiation and long-term depression. *J. Neurosci.* *24*, 9847–9861.
- Isope, P., and Murphy, T.H. (2005). Low threshold calcium currents in rat cerebellar Purkinje cell dendritic spines are mediated by T-type calcium channels. *J. Physiol.* *562*, 257–269.
- Jaffe, D.B., Johnston, D., Lasser-Ross, N., Lisman, J.E., Miyakawa, H., and Ross, W.N. (1992). The spread of Na<sup>+</sup> spikes determines the pattern of dendritic Ca<sup>2+</sup> entry into hippocampal neurons. *Nature* *357*, 244–246.
- Jahr, C.E., and Stevens, C.F. (1990). A quantitative description of NMDA receptor-channel kinetic behavior. *J. Neurosci.* *10*, 1830–1837.
- Kampa, B.M., Letzkus, J.J., and Stuart, G.J. (2006). Requirement of dendritic calcium spikes for induction of spike-timing-dependent synaptic plasticity. *J. Physiol.* *574*, 283–290.

- Kampa, B.M., Letzkus, J.J., and Stuart, G.J. (2007). Dendritic mechanisms controlling spike-timing-dependent synaptic plasticity. *Trends Neurosci.* 30, 456–463.
- Kao, J.P., and Tsien, R.Y. (1988). Ca<sup>2+</sup> binding kinetics of fura-2 and azo-1 from temperature-jump relaxation measurements. *Biophys. J.* 53, 635–639.
- Koester, H.J., and Sakmann, B. (1998). Calcium dynamics in single spines during coincident pre- and postsynaptic activity depend on relative timing of back-propagating action potentials and subthreshold excitatory postsynaptic potentials. *Proc. Natl. Acad. Sci. USA* 95, 9596–9601.
- Koester, H.J., and Sakmann, B. (2000). Calcium dynamics associated with action potentials in single nerve terminals of pyramidal cells in layer 2/3 of the young rat neocortex. *J. Physiol.* 529, 625–646.
- Kovalchuk, Y., Eilers, J., Lisman, J., and Konnerth, A. (2000). NMDA receptor-mediated subthreshold Ca<sup>2+</sup> signals in spines of hippocampal neurons. *J. Neurosci.* 20, 1791–1799.
- Larkum, M.E., Kaiser, K.M., and Sakmann, B. (1999a). Calcium electrogenesis in distal apical dendrites of layer 5 pyramidal cells at a critical frequency of back-propagating action potentials. *Proc. Natl. Acad. Sci. USA* 96, 14600–14604.
- Larkum, M.E., Zhu, J.J., and Sakmann, B. (1999b). A new cellular mechanism for coupling inputs arriving at different cortical layers. *Nature* 398, 338–341.
- Lee, S.H., Rosenmund, C., Schwaller, B., and Neher, E. (2000). Differences in Ca<sup>2+</sup> buffering properties between excitatory and inhibitory hippocampal neurons from the rat. *J. Physiol.* 525, 405–418.
- Lipscombe, D., Helton, T.D., and Xu, W. (2004). L-type calcium channels: the low down. *J. Neurophysiol.* 92, 2633–2641.
- Llinás, R., and Nicholson, C. (1971). Electrophysiological properties of dendrites and somata in alligator Purkinje cells. *J. Neurophysiol.* 34, 532–551.
- Llinás, R., and Hess, R. (1976). Tetrodotoxin-resistant dendritic spikes in avian Purkinje cells. *Proc. Natl. Acad. Sci. USA* 73, 2520–2523.
- Llinás, R.R., and Steriade, M. (2006). Bursting of thalamic neurons and states of vigilance. *J. Neurophysiol.* 95, 3297–3308.
- Losonczy, A., and Magee, J.C. (2006). Integrative properties of radial oblique dendrites in hippocampal CA1 pyramidal neurons. *Neuron* 50, 291–307.
- Magee, J.C., and Johnston, D. (1997). A synaptically controlled, associative signal for Hebbian plasticity in hippocampal neurons. *Science* 275, 209–213.
- Magee, J.C., Christofi, G., Miyakawa, H., Christie, B., Lasser-Ross, N., and Johnston, D. (1995). Subthreshold synaptic activation of voltage-gated Ca<sup>2+</sup> channels mediates a localized Ca<sup>2+</sup> influx into the dendrites of hippocampal pyramidal neurons. *J. Neurophysiol.* 74, 1335–1342.
- Mainen, Z.F., Malinow, R., and Svoboda, K. (1999). Synaptic calcium transients in single spines indicate that NMDA receptors are not saturated. *Nature* 399, 151–155.
- Major, G., Polsky, A., Denk, W., Schiller, J., and Tank, D.W. (2008). Spatiotemporally graded NMDA spike/plateau potentials in basal dendrites of neocortical pyramidal neurons. *J. Neurophysiol.* 99, 2584–2601.
- Maravall, M., Mainen, Z.F., Sabatini, B.L., and Svoboda, K. (2000). Estimating intracellular calcium concentrations and buffering without wavelength ratioing. *Biophys. J.* 78, 2655–2667.
- Markram, H., and Sakmann, B. (1994). Calcium transients in dendrites of neocortical neurons evoked by single subthreshold excitatory postsynaptic potentials via low-voltage-activated calcium channels. *Proc. Natl. Acad. Sci. USA* 91, 5207–5211.
- Markram, H., Helm, P.J., and Sakmann, B. (1995). Dendritic calcium transients evoked by single back-propagating action potentials in rat neocortical pyramidal neurons. *J. Physiol.* 485, 1–20.
- Markram, H., Lubke, J., Frotscher, M., and Sakmann, B. (1997). Regulation of synaptic efficacy by coincidence of postsynaptic APs and EPSPs. *Science* 275, 213–215.
- McKay, B.E., McRory, J.E., Molineux, M.L., Hamid, J., Snutch, T.P., Zamponi, G.W., and Turner, R.W. (2006). Ca<sub>v</sub>3 T-type calcium channel isoforms differentially distribute to somatic and dendritic compartments in rat central neurons. *Eur. J. Neurosci.* 24, 2581–2594.
- Milojkovic, B.A., Zhou, W.L., and Antic, S.D. (2007). Voltage and calcium transients in basal dendrites of the rat prefrontal cortex. *J. Physiol.* 585, 447–468.
- Miyakawa, H., Ross, W.N., Jaffe, D., Callaway, J.C., Lasser-Ross, N., Lisman, J.E., and Johnston, D. (1992). Synaptically activated increases in Ca<sup>2+</sup> concentration in hippocampal CA1 pyramidal cells are primarily due to voltage-gated Ca<sup>2+</sup> channels. *Neuron* 9, 1163–1173.
- Miyata, M., Finch, E.A., Khiroug, L., Hashimoto, K., Hayasaka, S., Oda, S.I., Inouye, M., Takagishi, Y., Augustine, G.J., and Kano, M. (2000). Local calcium release in dendritic spines required for long-term synaptic depression. *Neuron* 28, 233–244.
- Müller, W., and Connor, J.A. (1991). Dendritic spines as individual neuronal compartments for synaptic Ca<sup>2+</sup> responses. *Nature* 354, 73–76.
- Nakamura, T., Barbara, J.G., Nakamura, K., and Ross, W.N. (1999). Synergistic release of Ca<sup>2+</sup> from IP<sub>3</sub>-sensitive stores evoked by synaptic activation of mGluRs paired with backpropagating action potentials. *Neuron* 24, 727–737.
- Naraghi, M. (1997). T-jump study of calcium binding kinetics of calcium chelators. *Cell Calcium* 22, 255–268.
- Neher, E. (1998). Usefulness and limitations of linear approximations to the understanding of Ca<sup>++</sup> signals. *Cell Calcium* 24, 345–357.
- Neher, E., and Augustine, G.J. (1992). Calcium gradients and buffers in bovine chromaffin cells. *J. Physiol.* 450, 273–301.
- Nevian, T., and Sakmann, B. (2004). Single spine Ca<sup>2+</sup> signals evoked by coincident EPSPs and backpropagating action potentials in spiny stellate cells of layer 4 in the juvenile rat somatosensory barrel cortex. *J. Neurosci.* 24, 1689–1699.
- Nevian, T., and Sakmann, B. (2006). Spine Ca<sup>2+</sup> signaling in spike-timing-dependent plasticity. *J. Neurosci.* 26, 11001–11013.
- Ngo-Anh, T.J., Bloodgood, B.L., Lin, M., Sabatini, B.L., Maylie, J., and Adelman, J.P. (2005). SK channels and NMDA receptors form a Ca<sup>2+</sup>-mediated feedback loop in dendritic spines. *Nat. Neurosci.* 8, 642–649.
- Nishiyama, M., Hong, K., Mikoshiba, K., Poo, M.M., and Kato, K. (2000). Calcium stores regulate the polarity and input specificity of synaptic modification. *Nature* 408, 584–588.
- Noguchi, J., Matsuzaki, M., Ellis-Davies, G.C., and Kasai, H. (2005). Spine-neck geometry determines NMDA receptor-dependent Ca<sup>2+</sup> signaling in dendrites. *Neuron* 46, 609–622.
- Nowak, L., Bregestovski, P., Ascher, P., Herbet, A., and Prochiantz, A. (1984). Magnesium gates glutamate-activated channels in mouse central neurones. *Nature* 307, 462–465.
- Oakley, J.C., Schwandt, P.C., and Crill, W.E. (2001). Dendritic calcium spikes in layer 5 pyramidal neurons amplify and limit transmission of ligand-gated dendritic current to soma. *J. Neurophysiol.* 86, 514–527.
- Plant, K., Pelkey, K.A., Bortolotto, Z.A., Morita, D., Terashima, A., McBain, C.J., Collingridge, G.L., and Isaac, J.T. (2006). Transient incorporation of native GluR2-lacking AMPA receptors during hippocampal long-term potentiation. *Nat. Neurosci.* 9, 602–604.
- Rancz, E.A., and Häusser, M. (2006). Dendritic calcium spikes are tunable triggers of cannabinoid release and short-term synaptic plasticity in cerebellar Purkinje neurons. *J. Neurosci.* 26, 5428–5437.
- Regehr, W.G., and Tank, D.W. (1990). Postsynaptic NMDA receptor-mediated calcium accumulation in hippocampal CA1 pyramidal cell dendrites. *Nature* 345, 807–810.
- Regehr, W.G., and Tank, D.W. (1992). Calcium concentration dynamics produced by synaptic activation of CA1 hippocampal pyramidal cells. *J. Neurosci.* 12, 4202–4223.
- Reid, C.A., Fabian-Fine, R., and Fine, A. (2001). Postsynaptic calcium transients evoked by activation of individual hippocampal mossy fiber synapses. *J. Neurosci.* 21, 2206–2214.

- Remy, S., and Spruston, N. (2007). Dendritic spikes induce single-burst long-term potentiation. *Proc. Natl. Acad. Sci. USA* 104, 17192–17197.
- Roberts, W.M. (1993). Spatial calcium buffering in saccular hair cells. *Nature* 363, 74–76.
- Ross, W.N., and Werman, R. (1987). Mapping calcium transients in the dendrites of Purkinje cells from the guinea-pig cerebellum in vitro. *J. Physiol.* 389, 319–336.
- Sabatini, B.L., and Regehr, W.G. (1998). Optical measurement of presynaptic calcium currents. *Biophys. J.* 74, 1549–1563.
- Sabatini, B.L., and Svoboda, K. (2000). Analysis of calcium channels in single spines using optical fluctuation analysis. *Nature* 408, 589–593.
- Sabatini, B.L., Maravall, M., and Svoboda, K. (2001). Ca(2+) signaling in dendritic spines. *Curr. Opin. Neurobiol.* 11, 349–356.
- Sabatini, B.L., Oertner, T.G., and Svoboda, K. (2002). The life cycle of Ca(2+) ions in dendritic spines. *Neuron* 33, 439–452.
- Safo, P.K., and Regehr, W.G. (2005). Endocannabinoids control the induction of cerebellar LTD. *Neuron* 48, 647–659.
- Sarkisov, D.V., and Wang, S.S. (2008). Order-dependent coincidence detection in cerebellar Purkinje neurons at the inositol trisphosphate receptor. *J. Neurosci.* 28, 133–142.
- Scheuss, V., Yasuda, R., Sobczyk, A., and Svoboda, K. (2006). Nonlinear [Ca2+] signaling in dendrites and spines caused by activity-dependent depression of Ca2+ extrusion. *J. Neurosci.* 26, 8183–8194.
- Schiller, J., Helmchen, F., and Sakmann, B. (1995). Spatial profile of dendritic calcium transients evoked by action potentials in rat neocortical pyramidal neurons. *J. Physiol.* 487, 583–600.
- Schiller, J., Schiller, Y., Stuart, G., and Sakmann, B. (1997). Calcium action potentials restricted to distal apical dendrites of rat neocortical pyramidal neurons. *J. Physiol.* 505, 605–616.
- Schiller, J., Schiller, Y., and Clapham, D.E. (1998). NMDA receptors amplify calcium influx into dendritic spines during associative pre- and postsynaptic activation. *Nat. Neurosci.* 1, 114–118.
- Schiller, J., Major, G., Koester, H.J., and Schiller, Y. (2000). NMDA spikes in basal dendrites of cortical pyramidal neurons. *Nature* 404, 285–289.
- Schwaller, B., Meyer, M., and Schiffmann, S. (2002). 'New' functions for 'old' proteins: the role of the calcium-binding proteins calbindin D-28k, calretinin and parvalbumin, in cerebellar physiology. Studies with knockout mice. *Cerebellum* 1, 241–258.
- Schwartzkroin, P.A., and Slawsky, M. (1977). Probable calcium spikes in hippocampal neurons. *Brain Res.* 135, 157–161.
- Simon, S.M., and Llinás, R.R. (1985). Compartmentalization of the submembrane calcium activity during calcium influx and its significance in transmitter release. *Biophys. J.* 48, 485–498.
- Sjöström, P.J., Rancz, E.A., Roth, A., and Häusser, M. (2008). Dendritic excitability and synaptic plasticity. *Physiol. Rev.* 88, 769–840.
- Sobczyk, A., Scheuss, V., and Svoboda, K. (2005). NMDA receptor subunit-dependent [Ca2+] signaling in individual hippocampal dendritic spines. *J. Neurosci.* 25, 6037–6046.
- Soderling, T.R. (2000). CaM-kinases: modulators of synaptic plasticity. *Curr. Opin. Neurobiol.* 10, 375–380.
- Soler-Llavina, G.J., and Sabatini, B.L. (2006). Synapse-specific plasticity and compartmentalized signaling in cerebellar stellate cells. *Nat. Neurosci.* 9, 798–806.
- Spruston, N., Schiller, Y., Stuart, G., and Sakmann, B. (1995). Activity-dependent action potential invasion and calcium influx into hippocampal CA1 dendrites. *Science* 268, 297–300.
- Stevens, C.F., and Zador, A.M. (1998). Input synchrony and the irregular firing of cortical neurons. *Nat. Neurosci.* 1, 210–217.
- Stuart, G., Schiller, J., and Sakmann, B. (1997). Action potential initiation and propagation in rat neocortical pyramidal neurons. *J. Physiol.* 505, 617–632.
- Svoboda, K., Denk, W., Kleinfeld, D., and Tank, D.W. (1997). In vivo dendritic calcium dynamics in neocortical pyramidal neurons. *Nature* 385, 161–165.
- Svoboda, K., Helmchen, F., Denk, W., and Tank, D.W. (1999). Spread of dendritic excitation in layer 2/3 pyramidal neurons in rat barrel cortex in vivo. *Nat. Neurosci.* 2, 65–73.
- Takechi, H., Eilers, J., and Konnerth, A. (1998). A new class of synaptic response involving calcium release in dendritic spines. *Nature* 396, 757–760.
- Tank, D.W., Sugimori, M., Connor, J.A., and Llinás, R.R. (1988). Spatially resolved calcium dynamics of mammalian Purkinje cells in cerebellar slice. *Science* 242, 773–777.
- Thiagarajan, T.C., Lindskog, M., and Tsien, R.W. (2005). Adaptation to synaptic inactivity in hippocampal neurons. *Neuron* 47, 725–737.
- Tsay, D., Dudman, J.T., and Siegelbaum, S.A. (2007). HCN1 channels constrain synaptically evoked Ca2+ spikes in distal dendrites of CA1 pyramidal neurons. *Neuron* 56, 1076–1089.
- Vicini, S., Wang, J.F., Li, J.H., Zhu, W.J., Wang, Y.H., Luo, J.H., Wolfe, B.B., and Grayson, D.R. (1998). Functional and pharmacological differences between recombinant N-methyl-D-aspartate receptors. *J. Neurophysiol.* 79, 555–566.
- Wang, S.S., Denk, W., and Häusser, M. (2000). Coincidence detection in single dendritic spines mediated by calcium release. *Nat. Neurosci.* 3, 1266–1273.
- Watanabe, S., Hong, M., Lasser-Ross, N., and Ross, W.N. (2006). Modulation of calcium wave propagation in the dendrites and to the soma of rat hippocampal pyramidal neurons. *J. Physiol.* 575, 455–468.
- Waters, J., Larkum, M., Sakmann, B., and Helmchen, F. (2003). Supralinear Ca2+ influx into dendritic tufts of layer 2/3 neocortical pyramidal neurons in vitro and in vivo. *J. Neurosci.* 23, 8558–8567.
- Wei, D.S., Mei, Y.A., Bagal, A., Kao, J.P., Thompson, S.M., and Tang, C.M. (2001). Compartmentalized and binary behavior of terminal dendrites in hippocampal pyramidal neurons. *Science* 293, 2272–2275.
- Westenbroek, R.E., Ahljianian, M.K., and Catterall, W.A. (1990). Clustering of L-type Ca2+ channels at the base of major dendrites in hippocampal pyramidal neurons. *Nature* 347, 281–284.
- Yasuda, R., Sabatini, B.L., and Svoboda, K. (2003). Plasticity of calcium channels in dendritic spines. *Nat. Neurosci.* 6, 948–955.
- Yuste, R., and Denk, W. (1995). Dendritic spines as basic functional units of neuronal integration. *Nature* 375, 682–684.
- Yuste, R., Gutnick, M.J., Saar, D., Delaney, K.R., and Tank, D.W. (1994). Ca2+ accumulations in dendrites of neocortical pyramidal neurons: an apical band and evidence for two functional compartments. *Neuron* 13, 23–43.
- Yuste, R., Majewska, A., Cash, S.S., and Denk, W. (1999). Mechanisms of calcium influx into hippocampal spines: heterogeneity among spines, coincidence detection by NMDA receptors, and optical quantal analysis. *J. Neurosci.* 19, 1976–1987.
- Zhou, Z., and Neher, E. (1993). Mobile and immobile calcium buffers in bovine adrenal chromaffin cells. *J. Physiol.* 469, 245–273.
- Zucker, R.S. (1999). Calcium- and activity-dependent synaptic plasticity. *Curr. Opin. Neurobiol.* 9, 305–313.